CORNER LOADING AND CURLING STRESS ANALYSIS OF CONCRETE PAVEMENTS

Ying-Haur Lee, Ying-Ming Lee, and Shao-Tang Yen
Department of Civil Engineering
Tamkang University
Taipei, Taiwan 251, R.O.C.
E-mail: yinghaur@tedns.te.tku.edu.tw.

ABSTRACT

Since corner breaks are one of the major structural distresses in jointed concrete pavements, this research study focuses on the determination of the critical bending stresses at the corner of the slab due to the individual and combination effects of wheel loading and thermal curling. A well-known slab-on-grade finite element program (ILLI-SLAB) was used for the analysis. The structural response characteristics of a slab corner were first investigated in this study. Secondly, comparison of the actual field measurements of the test sections of Taiwan's North Second Freeway with the resulting ILLI-SLAB stresses also showed fairly good agreements in its applicability for field stress estimation. Based on the principles of dimensional analysis, the dominating mechanistic variables were carefully identified and verified. The resulting ILLI-SLAB corner stresses were compared to theoretical Westergaard solutions. Adjustment factors (R) were introduced to account for this discrepancy. Prediction models were developed as an alternative to the very time-consuming and complicated F.E. analysis to estimate stresses for design purposes with sufficient accuracy. A numerical example showing the use of the models was also provided.

INTRODUCTION

Cracking of jointed concrete pavements (JCP) is often caused by three different critical repeated loading positions: transverse joint, longitudinal joint midway between transverse joints, and at the corner. Given certain design, construction, and loading conditions, any of these load positions could lead to fatigue cracking of the slab over time. "**Load repetition combined with loss of support and curling stresses**" are usually recognized as the main causes for corner breaks. Thus, this paper mainly focuses on the determination of critical bending stresses **at the corner** due to loading and curling.

Two methods are often used to determine the stresses and deflections in concrete pavements: closed-form formulas and finite element (F. E.) computer programs. The formulas originally developed by Westergaard are for a single wheel load under the assumptions of infinite slab size and full contact between the slab-subgrade interface. To more accurately and realistically account for the effects of a finite slab size and possible loss of subgrade support due to a temperature differential, F. E. analyses should be used. Nevertheless, the difficulties of the required run time and complexity often prevent it from being used in practical pavement designs.

The main objective of this research work was to help develop an alternative stress determination process which can be incorporated into existing mechanistic-based design procedures with sufficient accuracy and efficiency for practical pavement designs.

CLOSED-FORM SOLUTIONS

Corner Loading

In the analysis of a slab-on-grade pavement system, Westergaard has presented closed-form solutions for three primary structural response variables, i.e., slab bending stress, slab deflection, and subgrade stress, due to a single wheel load based on medium-thick plate theory. Based on the assumptions of an infinite or semi-infinite slab over a dense liquid foundation (Winkler foundation), Westergaard applied a method of successive approximations and obtained the following equations for a circular corner loading condition (*I*):

$$\sigma_w = \frac{3P}{h^2}\left[1-\left(\sqrt{2}\frac{a}{\mathrm{a}}\right)^{0.6}\right] \quad , \quad \delta_w = \frac{P}{k\mathrm{a}^2}\left[1.1-0.88\left(\sqrt{2}\frac{a}{\mathrm{a}}\right)\right] \qquad \text{(Eq.1)}$$

Where σ_w is the critical corner stress, [FL^{-2}]; δ_w is the critical corner deflection, [L]; P is the total applied wheel load [F]; h is the thickness of the slab [L]; a is the radius of the applied load [L]; $\mathrm{a} = [Eh^3/(12*(1-\mu^2)*k)]^{0.25}$ is the radius of relative stiffness of the slab-subgrade system [L]; k is the modulus of subgrade reaction [FL^{-3}]; E is the modulus of elasticity of the concrete slab [FL^{-2}]; and μ is the Poisson's ratio of the concrete. Note that primary dimensions are represented by [F] for force and [L] for length. The distance to the point of maximum stress along the corner angle bisector was found to be roughly:

$$X_1 = 2\sqrt{\sqrt{2}a^4} \cong 2.38\sqrt{a^4} \qquad \text{(Eq.2)}$$

The above stress and deflection equations were derived using a simple approximate process and has been debated and led to numerous revisions such as those proposed by Bradbury, Kelly, Teller and Sutherland, Spangler, and Pickett over the years (*2*). Despite this argument, Ioannides et al. (*3*) later has indicated that the ILLI-SLAB F.E. results closely fall between those predicted by Westergaard and Bradbury. The ILLI-SLAB stresses are the **minor principal (tensile) stresses** occurring at the top fiber of the slab corner. Thus, Westergaard's approximation was still fairly good.

Thermal Curling

Considering curling stresses caused by a linear temperature differential on a concrete slab over a dense liquid foundation, Westergaard (*4*) developed equations for three slab conditions (i.e., infinite, semi-infinite, and an infinite long strip). The interior stress for an infinite slab is:

$$\sigma_0 = \frac{E\alpha\Delta T}{2(1-\mu)} \qquad \text{(Eq.3)}$$

Where σ_0 is the interior curling stress, [FL^{-2}]; α is the thermal expansion coefficient, [T^{-1}]; and ΔT is the temperature differential through the slab thickness, [T]. Primary dimensions are represented by [F] for force, [L] for length, and [T] for temperature.

Bradbury (*5*) later expanded Westergaard's bending stress solutions for a slab with finite dimensions in both transverse and longitudinal directions. The edge and interior curling stresses can be determined by:

$$\sigma_{ce} = \frac{CE\alpha\Delta T}{2} = \frac{E\alpha\Delta T}{2}\left[1-\frac{2\cos\beta\cosh\beta}{\sin 2\beta+\sinh 2\beta}(\tan\beta+\tanh\beta)\right]$$

$$\sigma_{ci} = \frac{E\alpha\Delta T}{2}\left[\frac{C_1+\mu C_2}{1-\mu^2}\right] \quad , \quad \beta = \frac{B}{\mathrm{a}\sqrt{8}} \qquad \text{(Eq.4)}$$

Where σ_{ce} , σ_{ci} are the edge and interior curling stresses, [FL^{-2}]; B is the finite slab width or length, [L]; and C_1 , C_2 are curling stress coefficients for the desired and perpendicular directions. However, there exists no explicit closed-form corner stress solutions.

Loading Plus Thermal Curling

Considering the combined effect of loading plus curling, Bradbury further analyzed the curling stress on a diagonal corner section located at or near the section at which the maximum loading stress occurs, i.e. the location determined by (Eq.2). Consequently, Bradbury derived the following approximate corner curling stress:

$$\sigma_{ct} = \frac{E\alpha\Delta T}{3(1-\mu)}\sqrt{\frac{a}{\mathrm{a}}} \qquad \text{(Eq.5)}$$

Where σ_{ct} is the maximum curling stress to be combined with maximum stress induced by load at the corner, [FL^{-2}]. Even though Westergaard and Bradbury all suggested that this effect could be treated as "a simple mater of addition" in most cases, many investigators have indicated that such an action may not always be conservative (*3, 6*) due to the possible loss of subgrade support and violation of full contact assumptions.

F.E. COMPUTER PROGRAM

The analysis of finite slab length and width effect was not possible until the introduction of finite element models. The basic tool for this analysis is the ILLI-SLAB F.E. computer program which was originally developed in 1977 and has been continuously revised and expanded at the University of Illinois over the years. The ILLI-SLAB model is based on classical medium-thick plate theory, and employs the 4-noded 12-degree-of-freedom plate bending elements. The Winkler foundation assumed by Westergaard is modeled as a uniform, distributed subgrade through an equivalent mass foundation. Curling analysis was not implemented until versions after June 15, 1987.

The present version (March 15, 1989) (*6*) was successfully complied on available Unix-based workstations of the Civil Engineering Department at Tamkang University. With some modifications to the original codes, a micro-computer version of the program was also developed using Microsoft FORTRAN PowerStation (*7*).

CHARACTERISTICS OF CORNER STRESSES

The structural response characteristics of a slab subjected to the individual and combination effects of a single-wheel corner load and a linear temperature differential were first investigated. A preliminary analysis under this study has also indicated that the location of the maximum combined stress due to loading plus curling varies from case to case. Thus, unlike the analysis of interior or edge stresses where the maximum stresses occur in the same critical center or mid-slab location, the analysis of corner stresses is probably the most difficult one among these three cases. As illustrated in Figure 1 (a), the following parameters were also assumed:

$L/\ell = 7$	$W/\ell = 7$	$\ell = 41.86$ in.	$h = 12$ in.
$k = 240$ pci	$E = 5$ Mpsi	$\gamma = 0.087$pci	$\mu = 0.15$

Note that $a/\ell = 0.1$ and $c = 7.5$ in. were selected for the given single-wheel corner load and $\Delta T = -20$ ^{o}F and $\alpha = 5.5E\text{-}06$ /^{o}F were chosen for the temperature differential.

Loading Only

Under this case study, a tire pressure (p) of 78 psi was selected and the loaded area was equal to 7.5*7.5 in.^{2}. The resulting maximum tensile stress was 63.7 psi, located at (x, y) = (22.3in., 22.3in.) position. This point is equivalent to a distance of 31.1 in. along the corner angle bisector. According to Westergaard's equation (Eq.1), the corresponding maximum corner stress was 63.2 psi at a distance of X_1=31.7 in. Thus, the ILLI-SLAB results agree with Westergaard's solutions very well for this case.

Upward Curling Only

In this case, $\Delta T = -20$ ^{o}F and $\alpha = 5.5E\text{-}06$ /^{o}F were assumed. A more realistic assumption of partial contact between the slab-subgrade interface was allowed and the self-weight of the concrete slab was also considered. For the night-time condition when the temperature on the top of the slab was less than the bottom of the slab (or $\Delta T < 0$), an upward curling was occurred. Due to the slab's self-weight, tensile stresses occurred on the top and compressive stresses at the bottom of the slab. It is worth mentioning, however, that the maximum tensile stress (269.88 psi) occurred at the center of the slab rather than the corner.

Large Loading Plus Small Curling

Just to illustrate the combination effect, a relatively large and hypothetical tire pressure of p = 780 psi together with the same temperature differential were assumed in this case. Since nighttime (negative

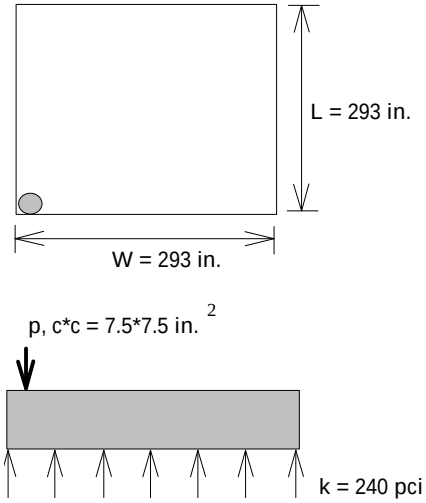

(a) Case Study of Corner Stress Analysis

(b) Loading Only

(c) Curling Only (Night-time Condition)

(d) Large Loading Plus Small Curling

(e) Small Loading Plus Large Curling

(f) Medium Loading Plus Medium Curling

Figure 1 - Distribution of the Tensile Stresses on the Top of the Slab

ΔT) curling condition will result in additional tensile stress at the top fiber of the slab, this study is only limited to the most critical case of corner loading plus night-time curling. The resulting maximum tensile stress was 683.73 psi, located at (x, y) = (4 in., 40 in.) position, which is equivalent to a distance of 40.2 in. along the corner angle bisector. This result is approximately equal to the sum of 10 times of the stress due to the loading-only case (p = 78 psi) and the tensile stress at the specified point due to curling alone.

Small Loading Plus Large Curling

This case assumes a tire pressure of p = 78 psi together with the same negative linear temperature differential. The resulting maximum tensile stress was 290.4 psi, located at (139 in., 139 in.) which is equivalent to a distance of X_1 = 196.6 in. along the diagonal line. In fact, it was very close to the center of the slab and the magnitude of the stress was approximately equal to the sum of both individual effects at that point.

Medium Loading Plus Medium Curling

This case assumes a tire pressure of p = 203 psi such that the resulting loading-only stress will have about the same magnitude as the aforementioned curling-only effect. The resulting maximum combined tensile stress was 306.2 psi, located at (120 in., 120 in.). This critical stress location was far away from the point of X_1 = 31.7 in. as determined by Westergaard's equation. The resulting maximum tensile stress was less than the summation of both individual effects using the principle of superposition.

Location of the Maximum Combined Stresses

The individual and combined stress contour plots of all cases were shown in Figure 1 (b) - (f), respectively. In summary, if the temperature differential is relatively small combined with a large corner load, the critical stress location is very close to Westergaard's maximum load stress location (Eq.2). However, if the temperature differential is very large along with a very small corner load, the critical stress location may shift toward and up to the center of the slab. For the combined effects of medium loading and medium curling, the maximum stress location falls between them. Thus, the location of the maximum combined stresses due to loading plus curling will fall within the Westergaard's location and the center of the slab along the corner angle bisector as shown in Figure 2. Furthermore, the corner stress along the line of a 1/4 circle centered at the very corner of the slab also shows about the same magnitude at most locations. This may help to explain the mechanism of the development of corner breaks as well.

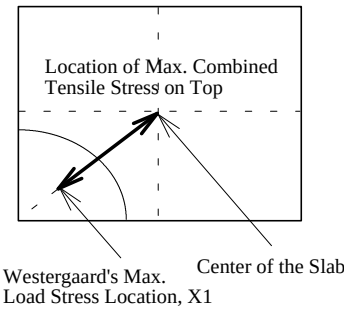

Figure 2 - Expected Maximum Combined Stress Location

Research continues with special attentions to this different critical stress location problem. Consequently, necessary modifications were made to the existing ILLI-SLAB codes to facilitate the search of critical stresses and locations alone the corner angle bisector or the diagonal nodes up to the center of the slab for the remaining analyses.

RESULTS OF ACTUAL FIELD MEASUREMENTS

To further investigate the applicability of the ILLI-SLAB F. E. program for stress estimation, the actual field measurements of the test sections of Taiwan's North Second Freeway (*8*) was obtained. The test sections were constructed as jointed concrete pavements (as illustrated in Figure 3) with an unbonded lean concrete base and the following characteristics: (Note: 1 in. = 2.54 cm, 1 psi = 0.07 kg/cm^2, 1 pci = 0.028 kg/cm^3, 1 kip = 454 kg)

1. finite slab size: 3-lane (one direction), L = 188 in., W = 148 in.
2. thickness of the top and the bottom layers: h_1 = 10 in., h_2 = 6 in.
3. concrete modulus of the top and the bottom layers: E_1 = 4.03E+06 psi, E_2 = 1.97E+06 psi
4. Poisson's ratio of the top and the bottom layers: $\mu_1 = \mu_2 = 0.20$
5. self-weight of the top and the bottom slabs: $\gamma_1 = \gamma_2 = 0.085$ pci
6. modulus of subgrade reaction: k = 481 pci
7. longitudinal joints: tied bars, spacing = 24 in., diameter = 5/8 in., Poisson's ratio = 0.2, elastic modulus = 2.9E+07 psi.
8. transverse joints: dowel bars, spacing = 12 in., diameter = 1.25 in., Poisson's ratio = 0.2, elastic modulus = 2.9E+07 psi, width of joint opening = 0.236 in., aggregate interlock factor (AGG) = 1000 psi, dowel concrete interaction (DCI) = 1.9E+06 lbs/in. (assumed).
9. with an AC outer shoulder.

A fully loaded truck with three different levels (60.7, 43.1, and 34.3 kips) of rear dual-tandem axle loads was placed near the slab corner. The gear configuration with the size of loaded area, wheel spacing and axle spacing was shown in Figure 3. At the time of testing, a positive temperature differential ΔT = 10.8 ºF was measured across the slab thickness; the slab thermal coefficient α was assumed 5.5E-06 /ºF.

The resulting horizontal stresses estimated by the ILLI-SLAB F. E. program were compared to the actual measured stresses near the slab corner and summarized in Table 1. Note that since the sensor locations C70 = (176.2 in., 11.8 in.), C71=(176.2 in., 74 in.), and C72=(176.2 in., 136.2 in.) was actually placed 2 in. below the slab surface, the resulting ILLI-SLAB stresses (compressive x-stress) were linearly adjusted (or reduced by 40%) while making such comparisons. As shown in Figure 4, fairly good agreements were achieved.

IDENTIFICATION OF DIMENSIONLESS MECHANISTIC VARIABLES

When there exist no closed-form solutions for the selected theoretical analysis tools or when analyzing most empirical but practical engineering problems, the use of the principles of dimensional analysis is often guaranteed. The principles of dimensional analysis treat a theoretical equation in non-dimensional form, which is comprised by a set of many dimensionless parameters representing a concise interrelationship among any complicated combinations of all input variables with dimensions. Thus, the number of parameters and data analysis time and costs may be reduced dramatically. This approach has also been widely accepted for engineering research.

Through the use of the principles of dimensional analysis, earlier investigators (*9*) have demonstrated that theoretical Westergaard solutions and F.E. solutions for three primary structural responses due to a single wheel load can be concisely defined by the following expression for a constant Poisson's ratio (usually $\mu \approx 0.15$):

$$\frac{\pm h^2}{P}, \frac{\delta k a^2}{P}, \frac{q a^2}{P} = f_1\left(\frac{a}{a}, \frac{L}{a}, \frac{W}{a}\right) \qquad \text{(Eq.6)}$$

Where σ, q are slab bending stress and vertical subgrade stress, respectively, [FL^{-2}]; δ is the slab deflection, [L]; f_1 is a function of *a*/a, L/a, and W/a; and L, W are finite slab length and width, [L]. Also Note that variables in both sides of the expression are all dimensionless. The dependent variables are σ

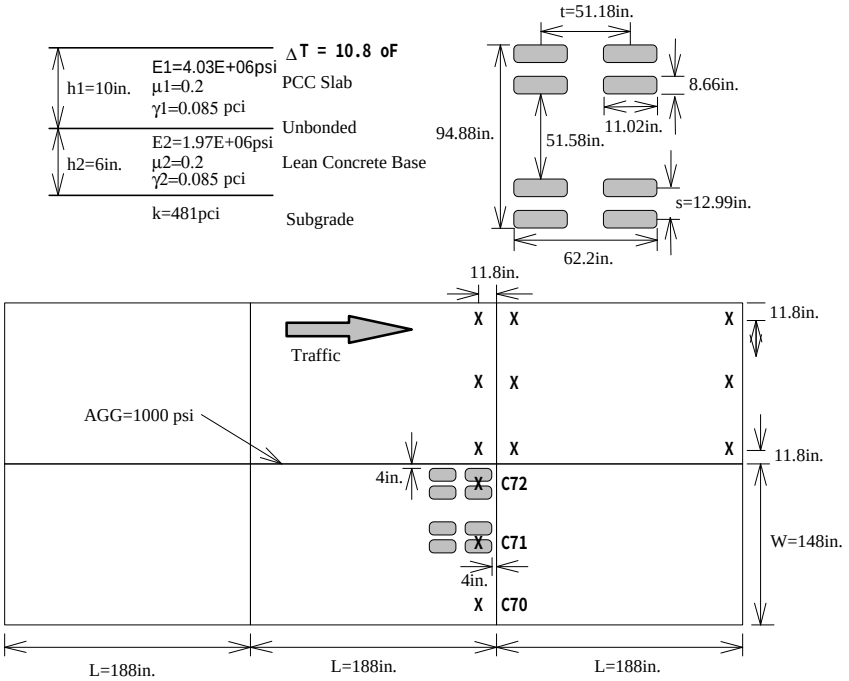

Figure 3 - A Case Study for Validation

Table 1 - Comparison of Measured versus ILLI-SLAB Estimated Stresses

Axle load (kips)	C 70		C 71		C 72	
	Measured (psi)	ILLI-SLAB (psi)	Measured (psi)	ILLI-SLAB (psi)	Measured (psi)	ILLI-SLAB (psi)
60.7	36.5	24.1	74.3	66.1	94.3	92.9
43.1	37.2	23.6	62.9	55.4	67.0	73.0
34.3	37.5	23.3	47.0	49.8	45.7	62.7

Figure 4 - Comparison Results of the Estimated versus Measured Stresses

h^2/P, $\delta k^{a2}/P$ and q^{a2}/P, which are only dominated by the normalized load radius (a/a), and the normalized slab length and width (L/a and W/a) rather than the other input parameters, such as E, h, k, a, etc.

Furthermore, according to recent research by Lee and Darter (*9*) for the stress analysis at the very edge of the slab, concise relationships have been proposed and numerically validated through a series of F.E. runs. The dimensionless mechanistic variables due to the effects of thermal curling alone and loading plus curling for a constant Poisson's ratio are:

$$\frac{\sigma}{E}, \frac{\delta h}{a^2}, \frac{qh}{ka^2} = f_2\left(\sim\Delta T, \frac{L}{a}, \frac{W}{a}, \frac{\gamma h^2}{ka^2}\right)$$

$$\frac{\sigma}{E}, \frac{\delta h}{a^2}, \frac{qh}{ka^2} = f_3\left(\frac{a}{a}, \sim\Delta T, \frac{L}{a}, \frac{W}{a}, \frac{\gamma h^2}{ka^2}, \frac{ph}{ka^4}\right)$$

$$D_\gamma = \frac{\gamma h^2}{ka^2}, \; D_p = \frac{ph}{ka^4} \qquad \text{(Eq.7)}$$

Where γ is the unit weight of the concrete slab, [FL^{-3}]; and f_2 , f_3 are functions for curling alone and curling plus loading, respectively. Also note that D_γ was defined as the relative deflection stiffness due to self-weight of the concrete slab and the possible loss of subgrade support, whereas D_p was the relative deflection stiffness due to the external wheel load and the loss of subgrade support. Conceptually, the above relationship should be applicable to any given loading conditions.

To numerically validate the above relationships for the individual and combined corner stresses due to loading and thermal curling in this study, several series of factorial F.E. runs were performed. For the case of loading only, 30 ILLI-SLAB runs as shown in Table 2 with the ranges for the dominating variables a/a = 0.05 ~ 0.3, L/a and W/a = 2 ~ 7 were conducted. Table 3 shows the other 20 different F.E. runs for the validation of loading plus curling. The data ranges are L/a, W/a = 2.6 ~ 15.5, a/a = 0.12 ~ 0.3, D_p = 5E-05 ~ 62.5E-05, D_γ = 2.7E-05 ~ 27E-05, and $\alpha\Delta T$ = -22E-05 ~ 20.4E-05. While keeping the dominating mechanistic variables constant but changing any other individual input variables to different values, the F.E. results have indicated that the aforementioned relationships also hold for the corner condition as expected.

CORNER STRESS PREDICTION MODELS

A series of F. E. factorial runs were performed based on the dominating mechanistic variables identified. Several BASIC programs were written to automatically generate the F. E. input files and summarize the desired outputs. The F. E. mesh was generated according to the guidelines established in earlier studies (*2*). As proposed by Lee and Darter (*10*), the projection pursuit regression (PPR) introduced by Friedman and Stuetzle (*11*) was used for the development of the following three stress prediction models. This algorithm is available in the S-PLUS statistical package (*12*).

1. CASE I (Loading only): Full contact assumption was applied, no temperature differential existed, and the self-weight of the slab was neglected.
2. CASE II (Loading plus curling, but $\Delta T = 0$): Partial contact between the slab-subgrade interface was allowed. Although the temperature differential was set to zero, the self-weight of the slab was considered in this case.
3. CASE III (Loading plus curling, but $\Delta T < 0$): A more general case for loading plus curling. Partial contact was allowed, and both the temperature differential and the slab's self-weight were considered.

The stress prediction models were represented in the form of adjustment factors (R), which were specially chosen to satisfy theoretical boundary conditions. As a result, R values range from 0 to 1, or at most up to an approximate maximum value of 1.2 for all three cases, which may also help to control the prediction accuracy.

Table 2 - Identification of Dimensionless Variables for Loading Only

W/ℓ	L/ℓ	a/ℓ	c	a	P	ℓ	L	W	E	k	h	σ	$\sigma h^2/P$
			in.	in.	psi	in.	in.	in.	Mpsi	pci	in.	psi	
2	2	0.3	5	2.821	2500	9.4	18.81	18.81	5	200	1.54	1061.7	1.007
2	2	0.3	5	2.821	2500	9.4	18.81	18.81	4	300	1.9	697.544	1.007
2	2	0.3	10	5.642	10000	18.81	37.61	37.61	3	400	5.81	294.72	0.995
2	2	0.3	10	5.642	10000	18.81	37.61	37.61	2	500	7.16	194.04	0.995
2	2	0.3	10	5.642	10000	18.81	37.61	37.61	1	650	9.84	102.73	0.995
3	3	0.3	5	2.821	2500	9.4	28.21	28.21	5	200	1.54	1377.62	1.307
3	3	0.3	5	2.821	2500	9.4	28.21	28.21	4	300	1.9	905.17	1.307
3	3	0.3	10	5.642	10000	18.81	56.42	56.42	3	400	5.81	379.52	1.281
3	3	0.3	10	5.642	10000	18.81	56.42	56.42	2	500	7.16	249.85	1.281
3	3	0.3	10	5.642	10000	18.81	56.42	56.42	1	650	9.84	132.26	1.281
4	4	0.1	5	2.821	2500	28.21	112.84	112.84	5	200	6.67	120.52	2.145
4	4	0.1	5	2.821	2500	28.21	112.84	112.84	4	300	8.23	79.17	2.145
4	4	0.1	10	5.642	10000	56.42	225.68	225.68	3	400	25.12	33.962	2.143
4	4	0.1	10	5.642	10000	56.42	225.68	225.68	2	500	30.97	22.343	2.143
4	4	0.1	10	5.642	10000	56.42	225.68	225.68	1	650	42.59	11.814	2.143
5	5	0.05	5	2.821	2500	56.42	282.09	282.09	5	200	16.81	21.748	2.458
5	5	0.05	5	2.821	2500	56.42	282.09	282.09	4	300	20.73	14.301	2.458
5	5	0.05	10	5.642	10000	112.84	564.19	564.19	3	400	63.29	6.135	2.457
5	5	0.05	10	5.642	10000	112.84	564.19	564.19	2	500	78.05	4.034	2.457
5	5	0.05	10	5.642	10000	112.84	564.19	564.19	1	650	107.32	2.134	2.458
6	6	0.3	5	2.821	2500	9.4	56.42	56.42	5	200	1.54	1464.98	1.390
6	6	0.3	5	2.821	2500	9.4	56.42	56.42	4	300	1.9	962.65	1.390
6	6	0.3	10	5.642	10000	18.81	112.84	112.84	3	400	5.81	401.49	1.355
6	6	0.3	10	5.642	10000	18.81	112.84	112.84	2	500	7.16	264.288	1.355
6	6	0.3	10	5.642	10000	18.81	112.84	112.84	1	650	9.84	139.894	1.355
4	7	0.2	5	2.821	2500	14.1	98.73	56.42	5	200	2.65	605.929	1.702
4	7	0.2	5	2.821	2500	14.1	98.73	56.42	4	300	3.27	398.03	1.702
4	7	0.2	10	5.642	10000	28.21	197.47	112.84	3	400	9.97	170.557	1.695
4	7	0.2	10	5.642	10000	28.21	197.47	112.84	2	500	12.29	112.229	1.695
4	7	0.2	10	5.642	10000	28.21	197.47	112.84	1	650	16.9	59.352	1.695

Note: While keeping W/l, L/l, and a/l constant, the resulting $\sigma h^2/P$ values still remain constant for any arbitrary combinations of all other parameters.

Table 3 - Identification of Dimensionless Variables for Loading Plus Curling

W/ℓ	L/ℓ	a/ℓ	c	P	ℓ	L	W	E	k	h	Dγ	Dp	ΔT	γ	σ	σ/E
			in.	psi	in.	in.	in.	Mpsi	pci	in.	x10^{-5}	x10^{-5}	^{o}F	pci	psi	x10^{-6}
2.6	5.5	0.12	2.5	469	11.75	64.65	30.56	5.3	200	2.04	7	25	-10	0.466	269.888	50.92
2.6	5.5	0.12	5	3608	23.51	129.29	61.12	4.2	300	6.35	7	25	-10	0.288	217.459	51.78
2.6	5.5	0.12	7.5	12126	35.26	193.94	91.68	3.5	400	12.75	7	25	-10	0.214	182.401	52.11
2.6	5.5	0.12	10	25559	47.02	258.59	122.24	2.1	500	23.9	7	25	-10	0.135	109.768	52.27
4.6	15.5	0.2	2.5	158	7.05	109.31	32.44	5.3	200	1.03	12	33	-40	1.124	666.448	125.74
4.6	15.5	0.2	5	1220	14.1	218.62	64.88	4.2	300	3.21	12	33	-40	0.694	527.171	125.52
4.6	15.5	0.2	7.5	4099	21.16	327.93	97.32	3.5	400	6.45	12	33	-40	0.516	439.146	125.47
4.6	15.5	0.12	10	33738	47.02	728.74	216.27	2.1	500	23.9	12	33	-40	0.232	263.277	125.37
5.6	5.6	0.3	2.5	8	4.7	26.33	26.33	5.3	200	0.6	27	5	0	3.313	29.53	5.57
5.6	5.6	0.3	5	63	9.4	52.66	52.66	4.2	300	1.87	27	5	0	2.046	23.928	5.70
5.6	5.6	0.3	7.5	211	14.1	78.99	78.99	3.5	400	3.76	27	5	0	1.522	20.098	5.74
5.6	5.6	0.3	10	444	18.81	105.32	105.32	2.1	500	7.04	27	5	0	0.963	12.124	5.77
12.6	5.5	0.15	2.5	646	9.4	51.72	118.48	5.3	200	1.51	5	62.5	14	0.386	500.999	94.53
12.6	5.5	0.15	5	4975	18.81	103.43	236.96	4.2	300	4.71	5	62.5	14	0.239	401.07	95.49
12.6	5.5	0.15	7.5	16720	28.21	155.15	355.44	3.5	400	9.47	5	62.5	14	0.178	334.697	95.63
12.6	5.5	0.15	10	35242	37.61	206.87	473.92	2.1	500	17.75	5	62.5	14	0.112	200.969	95.70
2.6	4.5	0.23	2.5	165	6.13	27.6	15.94	5.3	200	0.86	2.7	50	37	0.278	257.668	48.62
2.6	4.5	0.23	5	1273	12.26	55.19	31.89	4.2	300	2.67	2.7	50	37	0.171	212.862	50.68
2.6	4.5	0.23	7.5	4278	18.4	82.79	47.83	3.5	400	5.36	2.7	50	37	0.127	179.184	51.20
2.6	4.5	0.23	10	9018	24.53	110.38	63.78	2.1	500	10.04	2.7	50	37	0.081	108.762	51.79

Note: While keeping W/l, L/l, a/l, $\alpha\Delta T$, D_p, and D constant, the resulting σ/E values still remain about the same for any arbitrary combinations of all other parameters. (α = 5.5E–06 /^{o}F)

CASE I: Loading Only

In CASE I, a single wheel load was applied at the slab corner alone. There was no thermal curling effect and the Westergaard's full subgrade support was assumed in this case. Based on previous investigation (*3*), Westergaard's infinite slab assumption may be achieved if the normalized slab length (L/^{a}) is equal to 5.0 or more. Thus, a more conservative value of 7.0 for both L/^{a} and W/^{a} was selected to ensure infinite slab condition. The following factorial F.E. runs were conducted:

a/^{a}: 0.05, 0.1, 0.2, 0.3; L/^{a}: 2, 3, 4, 5, 6, 7; W/^{a}: 2, 3, 4, 5, 6, 7 (L/^{a} ≧ W/^{a})

Since L/^{a} and W/^{a} are analogous, a total of 84 runs were only necessary if slab length was chosen to be greater than slab width. The resulting maximum corner stresses were obtained and compared to the Westergaard solution. The following prediction model was developed for the adjustment factor (R):

$$R = \frac{\pm_{I\,(CASE\,I)}}{\pm_{w}} = 1.030 + 0.030\Phi_1 + 0.045\Phi_2$$

$$\Phi_1 = 92.415 - 149.276(A1) + 59.747(A1)^2$$

$$\Phi_2 = \begin{cases} -6.034 + 23.128(A2) - 22.022(A2)^2 & if \quad A2 \le 0.6 \\ -0.117 + 0.375(A2) & if \quad 0.6 < A2 \end{cases}$$

$$A1 = 0.8272x1 - 0.1219x2 + 0.0002x3 + 0.5485x4$$

$$A2 = -0.9034x1 + 0.2973x2 - 0.0118x3 - 0.3088x4$$

$$X1 = [x1, x2, x3, x4] = \left[\frac{a}{a}, \frac{L}{a} + \frac{W}{a}, \frac{L}{a} \times \frac{W}{a}, \sqrt{\frac{L}{a}} + \sqrt{\frac{W}{a}}\right] \qquad \text{(Eq.8)}$$

Statistics and Limits:

N = 84, R^2 = 0.980, SEE = 0.0081, CV = 0.79%, $0.05 \le a/^{a} \le 0.3, 2 \le L/^{a} \le 7, W/^{a} \le L/^{a}$

Note that N is the number of data points, R^2 is the coefficient of determination, SEE is the standard error of estimates, and CV is the coefficient of variation. This prediction model is also applicable to a larger slab when the upper bound value of 7.0 is used for the normalized slab length or width (L/^{a}, W/^{a}).

CASE II: Loading Plus Curling, but $\alpha\Delta T=0$

In CASE II, the combination effect of a single wheel load and a linear temperature differential (ΔT) at the slab corner was considered. **But, $\alpha\Delta T$ was assumed to be zero or very close to zero.** Therefore, the ILLI-SLAB program was modeled to allow partial contact between the slab-subgrade interface. Since a complete full factorial of all the six dimensionless parameters which requires a tremendous amount of computer time is not feasible. Thus, the following factorial F.E. runs were conducted:

a/ℓ: 0.05, 0.1, 0.2, 0.3; L/ℓ: 2, 3, 4, 5, 7, 9, 11, 13, 15; $W/\ell = L/\ell$; $\alpha\Delta T=0$

Notice that a square slab up to a maximum normalized slab length (L/ℓ) of 15, which may satisfy Westergaard's infinite slab assumption for thermal curling analysis. Furthermore, to account for D_{ℓ} and D_p effects without increasing the number of F.E. runs, the above factorial runs were randomized by these two factors for different a/ℓ values using the concept of experimental design. The corresponding values are given below:

a/ℓ	$(DG, DP) = (D_{\ell}, D_p)*10^5$
0.05	(1, 2) (10, 30) (7, 130)
0.10	(4, 30) (7, 70) (4, 130)
0.20	(4, 2) (7, 30) (10, 70)
0.30	(1, 2) (10, 70) (1, 130)

After conducting considerable amounts of PPR trials, the following predictive model was developed for the corner stress adjustment factor (R):

$$R = \frac{\sigma_{i\,(\text{CASE II})}}{\sigma_w} = 0.9949 + 0.17037\Phi_1 + 0.03020\Phi_2$$

$$\Phi_1 = \begin{cases} -0.85525 + 15.53557(A1) + 1.71139(A1)^2 & \text{if } (A1 \le 0.1) \\ 0.24816 + 0.28387(A1) - 0.06692(A1)^2 & \text{if } (A1 > 0.1) \end{cases} \qquad \text{(Eq.9)}$$

$$\Phi_2 = \begin{cases} -0.93998 + 3.72027(A2) + 11.13839(A2)^2 & \text{if } (A2 \le 0.18) \\ -2.93892 + 16.93742(A2) & \text{if } (A2 > 0.18) \end{cases}$$

$$A1 = -0.95810x1 + 0.03604x2 + 0.28368x3 - 0.00231x4 - 0.00033x5 - 0.00236x6 - 0.00144x7 + 0.01621x8$$

$$A2 = 0.99699x1 - 0.02358x2 + 0.05534x3 - 0.00265x4 + 0.00055x5 + 0.01611x6 - 0.00041x7 - 0.04602x8$$

$$X = [x1, x2, \ldots x8]$$

$$= \left[\frac{a}{\ell}, \frac{L}{\ell}, \frac{a}{\ell} \times \frac{L}{\ell}, \frac{a}{\ell} \times DP, DP, DG, \frac{DP}{DG}, \frac{a}{\ell} \times DG\right]$$

Statistics and Limits:

$N = 108,\ R^2 = 0.962,\ SEE = 0.0096,\ 005 \le a/\ell \le 0.3,\ 2 \le L/\ell \le 15,$

$W/\ell = L/\ell,\ 1 \le DG \le 10,\ 2 \le DP \le 130,\ DG = D\ell \times 10^5,\ DP = Dp \times 10^5$

CASE III: Loading Plus Curling, but $\alpha\Delta T \neq 0$

CASE II and CASE III all consider the combination effect of a single wheel load and a linear temperature differential (ΔT) at the slab corner. **However, $\alpha\Delta T$ was assumed to be different from zero in CASE III.** Therefore, other than ΔT was selected differently, the aforementioned factorial design of F.E. runs for CASE II was also adopted for this case. The ΔT values was selected as follows:

ΔT: -10, -20, -30, -40 ^oF (α=5.5E-06 /^oF)

Thus, a total of 432 factorial F.E. runs were conducted for this analysis. The following adjustment factor (R) was carefully selected to account for the theoretical difference between CASE II and Westergaard's interior curling stress solutions:

$$R = \frac{\sigma_{i\,(CASE\,III)} - \sigma_{i\,(CASE\,II)}}{\sigma_o} \quad \text{or} \quad \sigma_{i\,(CASE\,III)} = \sigma_{i\,(CASE\,II)} + R \times \sigma_o \qquad \text{(Eq.10)}$$

Where σ_1 is the combined maximum F.E. corner stress, [FL^{-2}]; and σ_0 is defined by (Eq.3). By using the PPR algorithm, the following predictive model for R was developed:

$$R = 0.2548 + 0.3076\Phi_1 + 0.1058\Phi_2 + 0.05934\,\Phi_3$$

$$\Phi_1 = \begin{cases} -0.28987 + 0.02840(A1) & \text{if } A1 \le 0 \\ -0.22478 + 0.40575(A1) & \text{if } A1 > 0 \end{cases}$$

$$\Phi_2 = \begin{cases} -1.46318 + 0.39571(A2) + 0.00231(A2)^2 - 0.00155(A2)^3 & \text{if } A2 \le 15 \\ 5.06880 - 0.32371(A2) & \text{if } A2 > 15 \end{cases}$$

$$\Phi_3 = \begin{cases} 0.73250 + 0.74738(A3) & \text{if } A3 \le 0 \\ 0.68128 + 0.25940(A3) & \text{if } A3 > 0 \end{cases}$$

$$\begin{aligned} A1 = {} & -0.04291x1 + 0.56894x2 - 0.43915x3 + 0.05771x4 \\ & - 0.12609x5 + 0.02591x6 + 0.01885x7 - 0.15518x8 \\ & + 0.50270x9 - 0.01229x10 + 0.31315x11 - 0.00903x12 \\ & + 0.00649x13 + 0.28839x14 - 0.04413x15 + 0.03329x16 - 0.00002x17 \end{aligned}$$

$$\begin{aligned} A2 = {} & -0.02058x1 + 0.83621x2 - 0.36689x3 + 0.25029x4 \\ & - 0.16713x5 + 0.04484x6 + 0.07580x7 + 0.03647x8 \\ & - 0.09497x9 + 0.00207x10 - 0.04534x11 - 0.00721x12 \\ & + 0.0007x13 + 0.23382x14 + 0.01217x15 + 0.01038x16 - 0.00016x17 \end{aligned}$$

$$\begin{aligned} A3 = {} & 0.04637\,x1 - 0.44327x2 + 0.39157x3 + 0.47010x4 \\ & - 0.12200x5 - 0.00537x6 - 0.00851x7 - 0.01246x8 \\ & - 0.48078x9 + 0.00443x10 + 0.01520x11 + 0.00322x12 \\ & - 0.00293x13 + 0.42430x14 + 0.01628x15 - 0.01370x16 + 0.00007x17 \end{aligned}$$

$$X = [x1, x2, \ldots\ldots, X17] = \begin{bmatrix} a/a,\ L/a,\ ADT,\ (a/a)*(L/a), \\ (a/a)*ADT,\ (L/a)*ADT, \\ (a/a)*(L/a)*ADT,\ DP,\ DG, \\ DP*DG,\ DP*(a/a),\ DP*(L/a), \\ DP*ADT,\ DG*(a/a),\ DG*(L/a), \\ DG*ADT,\ ADT*(L/a)*(a/a)*DP*DG \end{bmatrix} \qquad \text{(Eq.11)}$$

Statistics and Limits:

$N = 432,\ R2 = 0.951,\ SEE = 0.09,\ 0.05 \le a/a \le 0.3, 2 \le L/a \le 15, W/a = L/a,$

$1 \le DG \le 10, 2 \le DP \le 130, 5.5 \le ADT \le 22,\ DG = D¥ \times 10^5,\ DP = Dp \times 10^5,\ ADT = - \sim \times\ \Delta T \times 10^5$

VALIDATION OF STRESS PREDICTIONS

To further validate the applicability of the proposed prediction models for all three cases, a totally separate set of database was created using the following input parameters: E = 3.0, 5.5, 8.0 Mpsi; k = 50, 250, 500 pci; L =120, 240, 360 in.; h = 8, 12, 16 in.; ΔT = 0, -20, -30, -40°F (α = 5.5E-06 /°F). Note that the other pertinent input parameters are: c = 10 in., a = 5.642 in., P = 9000 lbs, p = 90 psi, $\mu = 0.15$, $\gamma = 0.087$ pci, and W = L.

This will result in a total of 81 ILLI-SLAB runs with the ranges of a/a = 0.07 ~ 0.21, L/a and W/a = 1.4 ~ 15.9 for Case I and Case II, and a total of 243 ILLI-SLAB runs for Case III. When the values are outside the specified limits of the prediction model, the upper or lower bounds were applied for the analysis. The predicted stresses were plotted against the resulting ILLI-SLAB corner stresses (*13*) as shown in Figure 5 (a) - (c), respectively. Apparently, almost perfect agreement of the stress predictions for Case I and Case II, and fairly good agreement for Case III were achieved. Thus, the applicability of the prediction models were further verified.

There exists, however, some minor discrepancy for Case III due to the fact that the critical location of minor principal stress changes from case to case. Thus, the location of critical stress occurrence should be further investigated for future improvement.

(a) Loading Only

(b) Loading Plus Curling, but $\Delta T=0$

(c) Loading Plus Curling, but $\Delta T<0$

Figure 5 - Validation of Corner Stress Predictions

A NUMERICAL EXAMPLE

Consider a pavement slab with the following characteristics: E = 3 Mpsi, k = 400 pci, L = 141 in., W = 141 in., h = 9.97 in., γ = 0.224 pci, μ = 0.15, and α = 5.5E-06 /°F. A single wheel load of 7,624 lbs with a loaded rectangle of the size of 10x10 in^2 is applied at the slab corner. A linear temperature differential of -10 °F (night-time curling) exists through the slab. Determine the critical corner stresses due to loading alone, and loading plus curling. (Note: 1 psi = 6.89 kPa, 1 pci = 0.27 MN/m^3, 1 in. = 2.54 cm, 1 °F = (F - 32) / 1.8 °C, 1 lb = 4.45 N.)

The equivalent radius of the loaded area is a = 5.64 in. and the radius of relative stiffness of the slab-subgrade system is l = 28.21 in. Therefore, the dimensionless mechanistic variables are a/ℓ = 0.2, L/ℓ = W/ℓ = 5, ADT = 5.5, DG = 7, and DP = 30. The Westergaard solutions are σ_w = 122.3 psi and σ_0 = 97.1 psi for loading and curling alone using (Eq.1) and (Eq.3).

For the case of loading only, the adjustment factor R = 1.054 using (Eq.8). Thus, the corner stress determined by the proposed model is 1.062 x 122.3 = 129.9 psi. (Note that the actual ILLI-SLAB stress was 129.1 psi.)

For the case of loading plus curling, the adjustment factors for Case II and Case III are R = 1.054 and 0.139 using (Eq.9) and (Eq.11), respectively. Thus, the predicted total corner stress determined by the proposed model is 1.054 * 122.3 + 0.139 * 97.1 = 142.4 psi using (Eq.10). (Note that the actual ILLI-SLAB corner stress was 147.5 psi for this case.)

CONCLUSIONS

The corner stress of a concrete slab due to the individual and combination effects of loading and night-time curling was conducted under this study. A linear temperature differential across the slab thickness and a dense liquid foundation were assumed. The structural response characteristics of a slab corner were first investigated in this study. Secondly, comparison of the actual field measurements of the test sections of Taiwan's North Second Freeway with the resulting ILLI-SLAB stresses also showed fairly good agreements in its applicability for field stress estimation.

Based on the principles of dimensional analysis, six dimensionless mechanistic variables which dominate the primary structural responses were used for the analysis. A new modeling procedure was utilized to develop stress prediction models. The prediction models were properly formulated to satisfy applicable engineering boundary conditions. The models not only cover almost all practical ranges of pavement designs, but they are also dimensionally correct. These models can be implemented as a part of a design procedure to the very time-consuming and complicated F.E. analysis to estimate stresses for design purposes with efficiency and sufficient accuracy. A numerical example showing the use of the models was also provided.

ACKNOWLEDGMENTS

This research work was sponsored by the National Science Council, the Republic of China, under the grant No. NSC84-2211-E032-022. Professor Ping-Shien Lin and Mr. Yuan-Ting Wu are greatly acknowledged for providing and helping the interpretation of the results of the Test Sections.

REFERENCES

1. Westergaard, H. M. (1926a). "Computation of Stresses in Concrete Roads." Proceedings, Fifth Annual Meeting, Vol. 5, Part I, Highway Research Board.
2. Ioannides, A. M. (1984). "Analysis of Slabs-on-Grade for a Variety of Loading and Support Conditions." Ph.D. Thesis, University of Illinois, Urbana.
3. Ioannides, A. M., M. R. Thompson, and E. J. Barenberg (1985). "The Westergaard Solutions Reconsidered." Transportation Research Record 1043.
4. Westergaard, H. M. (1926b). "Analysis of Stresses in Concrete Pavements due to Variations of Temperature." Proceedings, Vol. 6, Highway Research Board.
5. Bradbury, R. D. (1938). Reinforced Concrete Pavements. Wire Reinforcement Institute, Washington, D.C.

6. Korovesis, G. T. (1990). "Analysis of Slab-on-Grade Pavement Systems Subjected to Wheel and Temperature Loadings." Ph.D. Thesis, University of Illinois, Urbana.
7. Microsoft (1994). "Microsoft FORTRAN PowerStation Professional Development System." User's and Reference Manuals, Microsoft Taiwan Corp.
8. Yen, Tsong, Ping-Sien Lin, et. al. (1993, 1994). "Practical Design Study of Rigid Pavements in Taiwan," Final Reports of Phase I and Phase II, Prepared for Taiwan Area National Expressway Engineering Bureau, Prepared by National Chung-Hsing University, Taiwan, R.O.C., 1993-1994 (in Chinese).
9. Lee, Y. H., and M. I. Darter (1994a). "Loading and Curling Stress Models for Concrete Pavement Design." Transportation Research Record 1449, pp. 101-113.
10. Lee, Y. H., and M. I. Darter (1994b). "New Predictive Modeling Techniques for Pavements." Transportation Research Record 1449, pp. 234-245.
11. Friedman, J. H. and W. Stuetzle (1981). "Projection Pursuit Regression." Journal of the American Statistical Association, Vol. 76, pp. 817-823.
12. Statistical Sciences, Inc. (1993). S-PLUS for Windows: User's and Reference Manuals. Ver. 3.1, Seattle, Washington.
13. Lee, Y. H. and Y. M. Lee (1995). "Theoretical Investigation of Corner Stress in Concrete Pavements Using Dimensional Analysis." Final Report, National Science Council, NSC83-0410-E032-009 and NSC84-2211-E032-022, Taiwan, R.O.C., (In Chinese).